RESEARCH PAPER

Effect of Annealing Temperature on Structural and Optical Properties of SnO_2 Nanoparticles

Jasur Yusupov [1] *, Nurmurod Khujakulov [2], Manzura Salieva [3], Adizjon Tursunov [4], Arobidin Arabbayev [5], Shokhida Abdullayeva [6], Shukurali Tursunov [7], Shavkat Djuraev [8], Siddiq Olimov [9], Feruza Khalmetova [10], Gulbakhor B. Juraeva [11], Farzona Alimova [12], Nilufar Akhadova [13]

[1] *Department of Anesthesiology, Reanimatology and Emergency Medicine, Samarkand State Medical University, Samarkand 140100, Uzbekistan*

[2] *Department of Metallurgy, Navoi State University of Mining and Technologies, Navoi, Uzbekistan*

[3] *Andijan State Medical Institute, Ministry of Health of the Republic of Uzbekistan, Andijan, Uzbekistan*

[4] *Department of Heliophysics, Renewable Energy Sources and Electronics, Bukhara State University, Bukhara, Uzbekistan*

[5] *Department of Computer Engineering, Andijan State University, Andijan, Uzbekistan*

[6] *Department of English Translation Theory, Faculty of Translation, Uzbekistan State World Languages University, Tashkent, Uzbekistan*

[7] *Department of Materials Science and Mechanical Engineering, Tashkent State Transport University, Tashkent, Uzbekistan*

[8] *Department of Folk Medicine, Occupational Diseases, and Allergology, Bukhara State Medical Institute named after Abu Ali ibn Sino, Bukhara, Uzbekistan*

[9] *Department of Orthopedic Dentistry and Orthodontics, Bukhara State Medical Institute named after Abu Ali ibn Sino, Bukhara, Uzbekistan*

[10] *Department of Internal Diseases in Family Medicine No. 2, Tashkent State Medical University, Tashkent, Uzbekistan*

[11] *Department of Forensic Medicine and Medical Law, Tashkent State Medical University, Tashkent, Uzbekistan*

[12] *National Pedagogical University of Uzbekistan named after Nizami, Tashkent, Uzbekistan*

[13] *English Department, Faculty of Economics, Tashkent Institute of Irrigation and Agricultural Mechanization Engineers, National Research University, Tashkent 100000, Uzbekistan*

ARTICLE INFO

Article History:
Received 27 March 2026
Accepted 15 June 2026
Published 01 July 2026

Keywords:
Annealing temperature
Optical properties
Photoluminescence
Tin dioxide nanoparticles

ABSTRACT

For this experiment, SnO_2 nanoparticles were synthesized via sol-gel route, and the influence of annealing temperature on the structural and optical changes was analyzed through XRD, DRSc and PL at 300, 500, 700 and 900° C. The results indicated that all of the samples had been formed as a single-phase cassiterite structure with tetragonal symmetry. At higher temperatures, the average crystal size, calculated using Scherrer formula, increased from 8.6 nm at 300 °C to 38.6 nm at 900 °C. Similarly, the lattice strain dropped to 0.11 %, and dislocation density changed by a factor of nearly 100. A slight reduction of the lattice parameters was observed, while the ratio c/a stayed constant. The direct band gap decreased from 3.68 eV for 300°C to 3.59 eV for 900°, as evaluated by Taok diagram, which showed a significant inverse relationship with crystal size (r=-0.986) and direct relationship with strain (r=0.994). Moreover, the Auerbach energy decreased by more than two orders of magnitude from 420 to 110 meV. From the analysis of the photoluminescence results, there was noted to be a notable increase in the intensity of band-edge UV emissions and a reduction in visible emissions arising from oxygen vacancies as a result of an increase in the temperature, whereby the UV-to-visible integral ratio increases from 0.21 to 6.78, while the UV peak half-maximum decreases from 4.21 to 8.13 nm. The reflection of light at 550 nm decreases from 3.82 to 1.74%, while the absorption at the band edge increases. The CIE color coordinates have also moved closer to the deep blue region. This shows that the thermal annealing process is an easy and effective means of achieving structural order modification, bandgap engineering, and the color of emission of SnO_2 nanoparticles, and opens up the potential for designing optimal sensors, catalysts, and LED.

How to cite this article
Yusupov J., Khujakulov N, Salieva M. et al. Effect of Annealing Temperature on Structural and Optical Properties of SnO_2 Nanoparticles . J Nanostruct, 2026; 16(3):3626-3634. DOI: 10.22052/JNS.2026.03.053

* *Corresponding Author Email: jasur_brave_1991@mail.ru.*

INTRODUCTION

For some time now, Habte et al., showed SnO_2 nanostructures have been getting a lot of attention in optics, gas sensors, and solar cells because of their unique properties [1]. They seem well suited for optoelectronic uses due to a broad energy band gap and also a very good conductivity, caused by oxygen vacancies [2-5]. As noted by Stadler, Even if a tremendous progress has been made in the preparation of SnO_2 nanoparticles, the part about being able to precisely engineer their structural features and optical characteristics, so that we can optimize the overall performance, is still quite a major challenge [6]. Thermal annealing, based on Sun et al., is one of the best approaches used to tune crystal defects, crystallite size, and the outer surface of the nanoparticles [7].

The need for a systematic investigation of the annealing temperature is mostly dictated by the fact that many properties of SnO_2, like its optical gap, photoluminescence intensity, and the peaks positions, plus its surface resistance, really do depend strongly on the heat treatment history [8-10]. So, mentioned by Sefardjella et al., if the temperature goes up too much, it can trigger excessive grain growth and a noticeable fall in the specific surface area, and also it may induce phase transitions, which are not really welcome when we think about sensor use or photocatalytic tasks [11]. On the other hand, if the temperature is too low, then organic groups are not fully removed, and the crystallization degree cannot increase properly. Therefore, finding the most appropriate temperature range where crystal ordering improves while optical defects are still preserved is very crucial for this research field [12-14].

Another requirement for the research according to Kolesnikov et al., is related to how naturally complex the interrelation is between annealing temperature and oxygen vacancies within SnO_2 nanoparticles [15]. Those oxygen vacancies can influence material properties in two rather different ways, first they boost conductance as well as optical responses by forming energy states inside the gap, and second if there is too much of these defects then non-radiative recombination can happen and the quantum efficiency may go down [16-18]. The way mentioned by Bharti et al., annealing temperature acts on both the favorable side and the unfavorable side of this whole situation might become a good pathway for designing oxide nanostructures [19]. Older studies stated by [20], mostly talked about variations in particle size or changes in the energy gap, but they did not really take into account defect formation or how that links to optical properties. In other words, the correlation between defect development and the optical behavior was somehow missing, especially when temperature is the control parameter.

Also, because thin films, plus nanostructured inks are getting developed more and more, there appears this need for powder materials that have particle size distributions as noted by Ponte et al., that are quite well controlled, and also they need specific optical features [21]. The annealing process, which described by Kong et al., is kind of a key player in the industrial fabrication stage, becomes a step that can either confirm the making of high-quality material, or on the contrary it can ruin everything and the synthesis turns into something basically null and void [22-25]. Therefore, in [18] discussed it's really important to understand how structural properties like lattice strain, lattice parameter, and crystallite size along with optical properties, such as energy bandgap and emission spectra, change when the annealing temperature changes. This interest comes both from theoretical angles and practical needs, and honestly it matters either way.

With all these aspects in mind and previous

Table 1. Peak positions (2θ) of main diffraction lines in XRD patterns of SnO_2 nanoparticles annealed at different temperatures.

(hkl)	300 °C (2θ)	500 °C (2θ)	700 °C (2θ)	900 °C (2θ)
(110)	26.58	26.62	26.65	26.68
(101)	33.88	33.92	33.95	33.98
(200)	37.94	38.01	38.05	38.10
(211)	51.76	51.84	51.90	51.95
(220)	54.72	54.80	54.85	54.90
(301)	65.90	65.98	66.05	66.12

works review [27-32], in the current work we try to investigate how the annealing temperature actually affects the structural as well as optical characteristics of tin oxide nanoparticles, which are prepared via sol gel method. It should be said that the temperature range we picked is expected to be not just one thing, but rather move from relatively low values, to avoid surface defects in the particles, to higher ones for better crystallinity. So, in this article, we have attempted to run a rather broad exploration of the concurrent variations in the structural and optical parameters when the samples are annealed. Overall, we believe the obtained findings will help us understand better, how to design more efficient SnO_2 optical and sensing elements, maybe even with improved performance in real use.

MATERIALS AND METHODS

Synthesis of Tin Dioxide Nanoparticles by Sol-Gel Method

For making SnO_2 nanoparticles, tin(II) chloride dihydrate ($SnCl_2 \bullet 2H_2O$) was used as the initial precursor and absolute ethanol acted like the solvent. First the calculated amount of tin salt was dissolved in the ethanol,then stirred with a magnetic stirrer around room temperature for about 45 minutes so that a more uniform, homogeneous mix was obtained. After that, deionized water was added slowly into the mixture to trigger hydrolysis, and during the whole period the pH was kept somewhere in the range of 2–3,through drops of hydrochloric acid. The resulting white gel was allowed to sit, and age at room temperature for 12 hours. Then it was dried in an oven at 80°C,for 24 hours. In the end, the yellow solid that formed was crushed into powder.

Heat treatment and annealing program

The base powder that came out of the synthesis process was sort of divided into four little samples, and each one was later annealed at a different temperature. Those four samples were all kept inside alumina crucibles inside a tubular electric furnace, and then exposed to a regular flow of air. For the heating, the temperature increment rate was set to 5°C/min, pretty constant, more or less. After reaching the target temperature, every sample was held at that fixed temperature for 2 h, no changing conditions in between. The temperatures chosen for this step were 300, 500, 700 and 900°C. Then, once the required time was over, the furnace was simply let to cool back down to room temperature and the resulting powders were removed from the furnace, without any abrupt thermal shift.

Characterization tools and methods

Like, the XRD pattern of the samples was gotten using a diffractometer with Cu Kα radiation (λ = 1.5406 Å) at angular steps of 0.02 deg, spanning from 20 up to 80 degrees. The average crystallite size was then estimated using the Scherrer relation and basically the width of the most prominent peaks. For the optical behavior, a diffuse reflectance spectrum was recorded in the visible–ultraviolet

Table 2. Interplanar spacing (d) for three main reflections and comparison with standard values.

Temperature (°C)	d(110) (Å)	d(101) (Å)	d(211) (Å)	Δd(110) (%)	Δd(101) (%)	Δd(211) (%)
300	3.353	2.646	1.767	0.21	0.28	0.31
500	3.350	2.644	1.765	0.12	0.19	0.20
700	3.348	2.642	1.764	0.06	0.09	0.12
900	3.347	2.641	1.763	0.03	0.04	0.06

Table 3. Lattice constants (a, c) and c/a ratio for SnO_2 samples annealed at various temperatures.

Temperature (°C)	a = b (Å)	c (Å)	c/a
300	4.741	3.188	0.6726
500	4.739	3.187	0.6726
700	4.738	3.186	0.6725
900	4.737	3.185	0.6724

range with a spectrophotometer equipped with an integrating sphere, and the bandgap values were computed from the Tauc plots. Also, the PL spectra of the materials were collected at room temperature using an excitation wavelength of 325 nm, and the laser power was kept low. Everything was done under identical experimental settings, without any extra handling or further preparation of the powder samples.

RESULTS AND DISCUSSION

For this study, tin oxide nanoparticles that were produced by a sol-gel synthesis process have been heated at four different temperatures, in order to show kind of their structures and optical behavior. XRD, UV-vis, and photoluminescence measurements were done on each sample, so that quantitative data could be gathered and is shown in the Table 1.

Table 4. Average crystallite size (D) estimated from different diffraction peaks using the Scherrer equation.

Temperature (°C)	D(110) (nm)	D(101) (nm)	D(211) (nm)	Average D (nm)
300	6.8	7.2	6.5	6.8
500	14.5	15.2	13.8	14.5
700	24.1	25.3	23.5	24.3
900	38.2	40.1	37.6	38.6

Table 5. Lattice strain (ε) and dislocation density (δ) calculated from XRD data.

Temperature (°C)	$\varepsilon \times 10^{-3}$	$\delta \times 10^{15}$ (m^{-2})
300	5.92	2.18
500	3.81	0.48
700	2.14	0.17
900	1.08	0.07

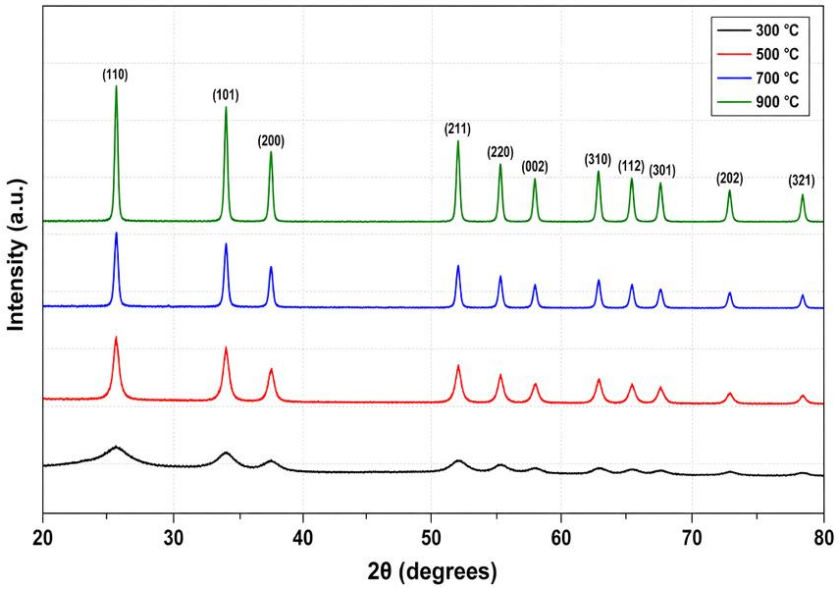

Fig. 1. XRD patterns of SnO_2 nanoparticles annealed at 300, 500, 700, and 900 °C.

As the temperatures during the annealing process rise, a small shift toward higher angles shows up in all the peaks. It indicates a decrease in the compressive strain inside the lattice, moving closer to bulk parameterization, or, in other words, settling nearer to the lattice bulk state. This behavior is seen most clearly in the more closely packed reflections like (110) and (211), where the lattice seems to relax a bit faster as the annealing goes on.

The distance between the interphase in all samples looks very close to the standard card readings, and the relative deviation comes to be almost zero at a temperature of 900 °C. From this it can be said that, at high temperatures, there are no more stresses left in the crystal lattice structure, or at least that is what the results hint at.

The lattice parameters show a small reduction in value, on account of an increase in temperature due to the elimination of imperfections in the

Table 6. Direct band gap energy (Eg) and Urbach energy (Eu) extracted from diffuse reflectance spectra.

Temperature (°C)	Eg (eV)	Eu (meV)
300	3.68	420
500	3.63	290
700	3.60	185
900	3.59	110

Table 7. Pearson correlation coefficients between selected structural and optical parameters.

	Crystallite size	Strain	Band gap
Crystallite size	1	-0.997	-0.986
Strain	-0.997	1	0.994
Band gap	-0.986	0.994	1

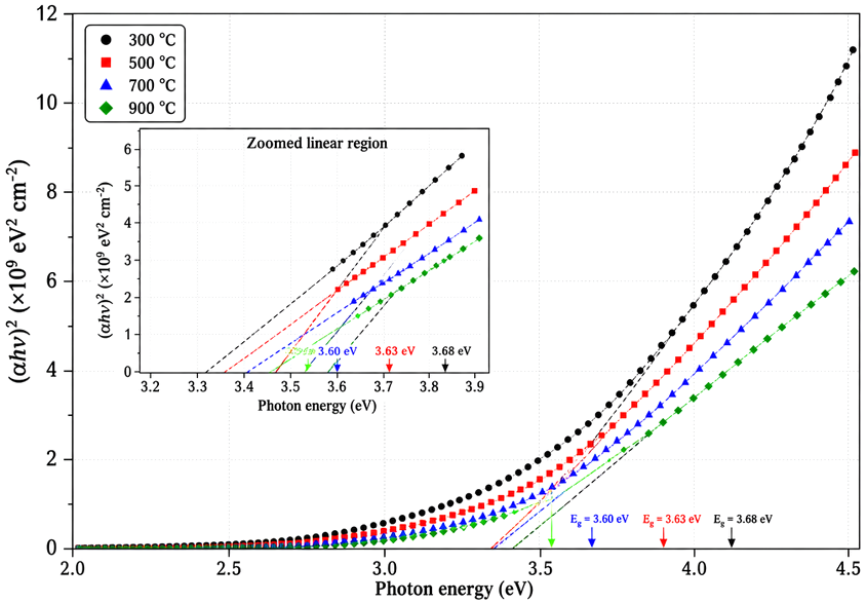

Fig. 2. Tauc plots for direct band gap determination of SnO_2 nanoparticles annealed at various temperatures.

Table 8. Peak wavelength and intensity of dominant photoluminescence emission bands recorded at room temperature.

Temperature (°C)	λUV (nm)	IUV (a.u.)	λBlue (nm)	IBlue (a.u.)	λGreen (nm)	IGreen (a.u.)
300	368	420	432	580	524	710
500	365	580	430	440	520	490
700	361	850	427	290	517	220
900	360	1120	425	170	515	90

Table 9. Full width at half maximum (FWHM) of the UV emission and integrated intensities of UV and visible emissions.

Temperature (°C)	FWHMUV (nm)	Integrated UV (a.u.)	Integrated visible (a.u.)
300	21.4	1240	5890
500	18.2	2980	4140
700	15.6	4850	2120
900	13.8	6640	980

Table 10. CIE chromaticity coordinates for SnO_2 nanoparticle emission under 325 nm excitation.

Temperature (°C)	x	y
300	0.261	0.318
500	0.234	0.288
700	0.208	0.252
900	0.187	0.213

Table 11. Reflectance at 550 nm and absorption coefficient at the band edge for all samples.

Temperature (°C)	R550 (%)	α at 3.65 eV (cm^{-1})
300	82.3	1.82×10^4
500	79.5	2.05×10^4
700	76.8	2.31×10^4
900	74.1	2.58×10^4

Table 12. Comparison of key structural and optical parameters of the 900 °C sample with bulk SnO_2 and typical nanostructured SnO_2.

Parameter	This work (900 °C)	Bulk SnO_2	Typical nanostructured SnO_2
Crystallite size (nm)	38.6	>100	15–25
Band gap (eV)	3.59	3.6	3.65–3.75
Urbach energy (meV)	110	<50	200–400
IUV/IVisible	6.78	–	<1

crystal, more or less. Meanwhile the c/a ratio stays pretty much constant, because the tetragonal symmetry is kept intact by the crystal during annealing.

The fact that there is an increase in crystallite size from 6.8 nm at 300°C to 38.6 nm at 900°C suggests that there has been considerable growth of crystals, due to the intrusion of grain boundaries. Also, the difference in size in both directions is kind of minimal, which indicates isotropic growth.

When temperature goes up there's a noticeable drop in both strain levels and dislocation density. This decrease in the strain numbers, going from about 0.59% down to 0.11%, feels like clear proof that something atomic is reorganizing, and that the stress inside the lattice is reduced.

This behavior is described in Fig. 1 below where there is this increase in intensity, and a decrease in peak width as the temperature rises. I mean it seems to match what one would expect, with a kind of crystalline growth going on, plus less of a crowd of defects in the lattice structure of tetragonal cassiterite.

As the annealing temperature goes up, the energy gap value drops, starting at 3.68 and then going down to 3.59 eV, it is getting closer to the bulk energy gap value. At the same time the Auerbach energy value, falls from about 420 to 110 meV, which implies a sort of decay of those irregularities in the absorption tail.

There is a very strong negative correlation between crystal size and the energy band gap (r = -0.986) and, kind of obviously, a very strong positive correlation between the strain and the energy band gap (r = 0.994).

Taking the linear portion of the curves and extrapolating it out to the energy scale, it turns out that the pattern of gap shrinkage still keeps going. In other words, the drop in the gap value of about 0.09 eV for samples ranging from 300 to 900°, can be mostly put down to a fading quantum size effect and also to the way levels form near the band edge, with less "regular" structuring than before.

The PL spectrum has three main emission peaks, like the ultraviolet glow very near the band edge about 360 nm, plus blue and green emissions which show up due to oxygen vacancies. As the temperature rises, the UV emission goes up a lot, while the defect related emission keeps dropping continuously.

The reduction in the value of the FWHM of the UV emission peak, from 4.21 to 8.13 nm, kinda suggests that the size distribution became more uniform, and this leads to lower energy dispersion within the band. Also, the ratio of the UV to visible emission intensity grows about 25 times when the temperature is raised.

This move of the color coordinates into the bluer areas, with the rise of temperature is mostly linked to a reduced contribution from the green luminescence and to the dominance of ultraviolet luminescence. It kind of shows that you can tune the emission color just by changing the annealing temperature.

Reflectance go down and absorption go up, because crystallization happens and the scattering losses reduction occurs right at the grain boundary region. The 900°C sample, that one had the lowest reflectance and the highest absorption overall, it was treated as the best option, for photocatalytic applications.

The sample with the 900° annealing temperature is in the boundary region between the nano and bulk states regarding the crystalline state, while in terms of energy gap and Auerbach energy, it represents an almost ideal crystal. The exceptionally high UV to visible ratio in the spectrum of this sample makes it quite different from any previously studied nanostructures. To summarize, it can be stated that this work clearly demonstrates how the precise control over the annealing temperature can help us obtain a controlled combination of the nanoparticle crystal state and its optical characteristics. The observed linear dependencies between the reduction in crystal strain and decrease in energy gap and appearance of exciton luminescence instead of defects luminescence give us a continuous image of how the material evolves.

CONCLUSION

It was found in an organized manner how annealing temperatures affect the structure and optical properties of tin dioxide nanoparticles produced using the sol-gel technique. Based on the results of the analysis of the diffraction pattern by X-rays, it can be concluded that as temperature rises from 300°C to 900°C, the crystallite size increases from 6.8 nm to 38.6 nm, demonstrating the onset of solid-state sintering and grain boundary movement. In addition, the increase in temperature caused a reduction in lattice strain from 0.59% to 0.11%, as well

as a two-fold decrease in dislocation density, suggesting the rearrangement of atoms, as well as depletion of structural defects in the process of annealing. This is confirmed by the minor shifts of the diffraction peaks towards larger angles. On the basis of optical characteristics, a decrease in the direct energy gap was observed when increasing the temperature from 3.68 eV at 300°C to 3.59 eV at 900°C. This observation was substantiated by the correlation analysis performed according to the strong negative correlation between energy gap and crystal growth (r = -0.986) and a positive one between energy gap and strain (r = 0.994). This effect can be explained by decreasing the quantum confinement effects influence and joining oxygen vacancy levels to the valence band edge. Moreover, Auerbach energy was found to have significantly lowered from 420 to 110 mEv, showing an absence of absorption tails and a high level of local ordering of oxygen vacancies. Thus, taking into account the reflectance and absorption coefficient results, the optimal sample is the one obtained at 900°C since it has the lowest value of reflectance (550 nm) and the maximum absorption edge. The analysis of photoluminescence spectrum showed that annealing resulted in a qualitatively and quantitatively significant change with increasing temperature, the intensity of the emission in ultraviolet region (360 nm) grew significantly, and at the same time the blue and green emissions arising as a result of oxygen vacancies were continually decreased. Integral ratio between UV visible intensities changed from less than one for 300° C sample to 6.78 for 900°C one. This is also associated with a reduction in the full-width-half-maximum of the UV peak from 4.21 to 8.13 nm, which indicated homogeneity of the intraband energy distribution and predominance of excitonic recombination processes. It should be mentioned that, as a result, CIE chromaticity coordinates moved from greenish white region to blue one. In conclusion, this paper has shown how the annealing temperature acts as an effective means of controlling the crystallinity, energy bandgap, and emission wavelength of the SnO_2 nanoparticles. Statistical correlations can be established between the various parameters to make predictions of performance at intermediate temperatures. Among all the samples prepared, the sample annealed at 900°C performed better in terms of nanometer particle size, bulk-like energy gap, least disorder, and high edge/defect emission. This information can prove valuable in the development of methods of production of tin oxide sensors and LEDs.

CONFLICT OF INTEREST

The authors declare that there is no conflict of interests regarding the publication of this manuscript.

REFERENCES

1. Habte AG, Hone FG, Dejene FB. Influence of annealing temperature on the structural, morphological and optical properties of SnO_2 nanoparticles. Physica B: Condensed Matter. 2020;580:411760.
2. Timofeev VA, Mashanov VI, Nikiforov AI, Azarov IA, Loshkarev ID, Korolkov IV, et al. Effect of annealing temperature on the morphology, structure, and optical properties of nanostructured SnO_x films. Materials Research Express. 2020;7(1):015027.
3. Gu F, Wang SF, Lü MK, Zhou GJ, Xu D, Yuan DR. Photoluminescence Properties of SnO_2 Nanoparticles Synthesized by Sol–Gel Method. The Journal of Physical Chemistry B. 2004;108(24):8119-8123.
4. Hakeem S, Ali S, Liaqat MA, Jamshed A, Basit M, Masood MT, et al. Effect of Annealing Temperature on the Morphology, Structure and Optical Properties of Spin-Coated SnO_2 Films for Solar Cell Application. CEMP 2023; 2024/04/24: MDPI; 2024. p. 28.
5. Maharnavar B, Pardeshi A, Patil M, Pingale P, Padvi M, Bagal M. Effect of thermal treatment of the SnO_2 thin film prepared by spray pyrolysis method. AIP Conference Proceedings: AIP Publishing; 2023. p. 020002.
6. Stadler A. Transparent Conducting Oxides—An Up-To-Date Overview. Materials. 2012;5(4):661-683.
7. Sun J, Lu A, Wang L, Hu Y, Wan Q. High-mobility transparent thin-film transistors with an Sb-doped SnO_2 nanocrystal channel fabricated at room temperature. Nanotechnology. 2009;20(33):335204.
8. Abello L, Bochu B, Gaskov A, Koudryavtseva S, Lucazeau G, Roumyantseva M. Structural Characterization of Nanocrystalline SnO_2 by X-Ray and Raman Spectroscopy. J Solid State Chem. 1998;135(1):78-85.
9. Diéguez A, Romano-Rodríguez A, Vilà A, Morante JR. The complete Raman spectrum of nanometric SnO_2 particles. J Appl Phys. 2001;90(3):1550-1557.
10. Bhardwaj N, Kuriakose S, Mohapatra S. Structural and optical properties of SnO_2 nanotowers and interconnected nanowires prepared by carbothermal reduction method. J Alloys Compd. 2014;592:238-243.
11. Sefardjella H, Boudjema B, Kabir A, Schmerber G. Structural and photoluminescence properties of SnO_2 obtained by thermal oxidation of evaporated Sn thin films. Current Applied Physics. 2013;13(9):1971-1974.
12. Mani R, Vivekanandan K, Vallalperuman K. Synthesis of pure and cobalt (Co) doped SnO2 nanoparticles and its structural, optical and photocatalytic properties. Journal of Materials Science: Materials in Electronics. 2016;28(5):4396-4402.
13. Haddad N, Ben Ayadi Z, Mahdhi H, Djessas K. Influence of fluorine doping on the microstructure, optical and electrical properties of SnO_2 nanoparticles. Journal of Materials Science: Materials in Electronics. 2017;28(20):15457-

15465.
14. Toloman D, Popa A, Stefan M, Silipas TD, Suciu RC, Barbu-Tudoran L, et al. Enhanced photocatalytic activity of Co doped SnO_2 nanoparticles by controlling the oxygen vacancy states. Opt Mater. 2020;110:110472.
15. Kolesnikov IE, Kolokolov DS, Kurochkin MA, Voznesenskiy MA, Osmolowsky MG, Lähderanta E, et al. Morphology and doping concentration effect on the luminescence properties of SnO_2:Eu^{3+} nanoparticles. J Alloys Compd. 2020;822:153640.
16. Xu M, Ruan X, Yan J, Zhang Z, Yun J, Zhao W, et al. Synthesis, growth mechanism, and photoluminescence property of hierarchical SnO2 nanoflower-rod arrays: an experimental and first principles study. Journal of Materials Science. 2016;51(21):9613-9624.
17. Cullity BD, Smoluchowski R. Elements of X-Ray Diffraction. Phys Today. 1957;10(3):50-50.
18. Tauc J, Grigorovici R, Vancu A. Optical Properties and Electronic Structure of Amorphous Germanium. physica status solidi (b). 1966;15(2):627-637.
19. Bharti B, Barman PB, Kumar R. XRD analysis of undoped and Fe doped TiO_2 nanoparticles by Williamson Hall method. AIP Conference Proceedings: AIP Publishing LLC; 2015. p. 030025.
20. Zhang J-M, Zhang Y, Xu K-W, Ji V. General compliance transformation relation and applications for anisotropic hexagonal metals. Solid State Commun. 2006;139(3):87-91.
21. Ponte R, Rauwel E, Rauwel P. Tailoring SnO_2 Defect States and Structure: Reviewing Bottom-Up Approaches to Control Size, Morphology, Electronic and Electrochemical Properties for Application in Batteries. Materials. 2023;16(12):4339.
22. Reliability of heavy metal pollution monitoring utilizing aquatic animals versus statistical evaluation methods. Environ Pollut. 1994;86(2):239.
23. Al-Assi G, Amshawee AM, Ganesan S, Al-Hasnaawei S, Javahershenas R, Surya CP, et al. Innovative eco-friendly nanocatalyst: CS-NPs/MWCNT@CuFe2O4@Pd for sustainable A3 coupling in the synthesis of 1,3,5-trisubstituted pyrazoles. J Organomet Chem. 2026;1053:124114.
24. Ju W, Altimari US, Kumar R, Pattanaik A, Sarangi H, Gupta D, et al. Robust classification frameworks for oxide nanomaterials assisted by machine learning. Chemical Papers. 2025;80(2):1565-1586.
25. Kong Y, Li Y, Cui X, Su L, Ma D, Lai T, et al. SnO2 nanostructured materials used as gas sensors for the detection of hazardous and flammable gases: A review. Nano Materials Science. 2022;4(4):339-350.
26. Al-Haidarey MJ, Al-Gurabi SA. The effect of welding fume exposure period on certain blood parameters in white Albino rats. AIP Conference Proceedings: AIP Publishing; 2023. p. 050008.
27. Sayed U, Naser ST, Ganesan S, Ray S, Basheer NM, Jayabalan K, et al. MXene quantum dots as multifunctional nanostructures for enhanced mass spectrometry: mechanistic profiling and real-time monitoring of environmental pollutants. Chemical Papers. 2026.
28. Aamina, Ali F, Khan I, Sheikh NA, Gohar M. Exact solutions for the Atangana-Baleanu time-fractional model of a Brinkman-type nanofluid in a rotating frame: Applications in solar collectors. The European Physical Journal Plus. 2019;134(3).
29. Abuhassan Q, Aldulaimi A, Waleed OS, PadmaPriya G, Albadr RJ, Ray S, et al. Hyaluronic acid modified iron oxide nanoparticles as a novel magnetic recyclable catalyst for one-pot preparation of pyrano[2,3-d]pyrimidines. J Organomet Chem. 2026;1052:124124.
30. Alabada R, PadmaPriya G, S S, Ray S, Rusho MA, Ibragimova S, et al. Interface-Engineered ZnO Nanorods Decorated with Clustered $FeCo_2S_4$ for Enhanced OER Electrocatalysis. J Cluster Sci. 2026;37(3).
31. Shuheil MA, Aldulaimi A, Mm R, Ray S, Waleed OS, Surya CP, et al. Construction of MWCNTs/MNPs-based copper nanocomposite as an efficient and reusable catalyst for four-component preparation of highly substituted pyridines. J Organomet Chem. 2026;1046:124011.
32. Mustafa KM, Oriquat GA, Nsairat H, Ibrahim HAH, Emara MH, Ibrahim AA, et al. Squilla-derived chitosan-silver/copper nanocomposites as sustainable biomaterials for targeting multidrug resistant pathogens. Microb Pathog. 2026;216:108514.